Slow magnetic relaxation in dinuclear Co(III)-Co(II) complexes containing a five-coordinated Co(II) centre with easy-axis anisotropy

Mengyao Liu,[a] Yimou Yang,[a] Rong Jing,[a] Shaojun Zheng,[a] Aihua Yuan,[a] Zhenxing Wang,*[b] Shu-Chang Luo,*[c] Xiangyu Liu,*[d] Hui-Hui Cui,[e] Zhong-Wen Ouyang[b] and Lei Chen*[a]

[a]School of Environmental and Chemical Engineering, Jiangsu University of Science and Technology, Zhenjiang 212003, P. R. China.

[b]Wuhan National High Magnetic Field Center & School of Physics, Huazhong University of Science and Technology, Wuhan 430074, P. R. China.

[c]School of Chemical Engineering, Guizhou University of Engineering Science, Bijie 551700, P. R. China.

[d]State Key Laboratory of High-efficiency Utilization of Coal and Green Chemical Engineering, National Demonstration Center for Experimental Chemistry Education, College of Chemistry and Chemical Engineering, Ningxia University, Yinchuan 750021, P. R. China.

[e]School of Chemistry and Chemical Engineering, Nantong University, Nantong 226019, P. R. China

Electronic Supplementary Information

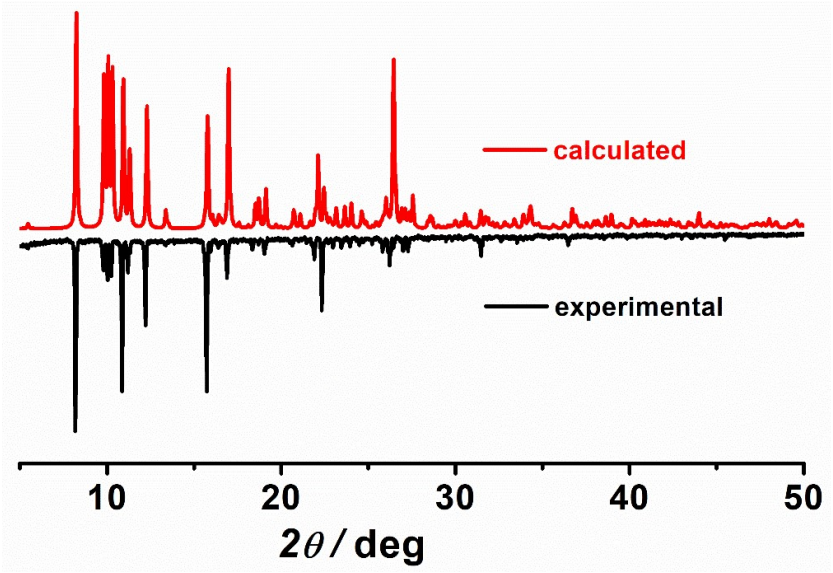

Figure S1. The powder X-ray diffraction pattern of **1** at room temperature.

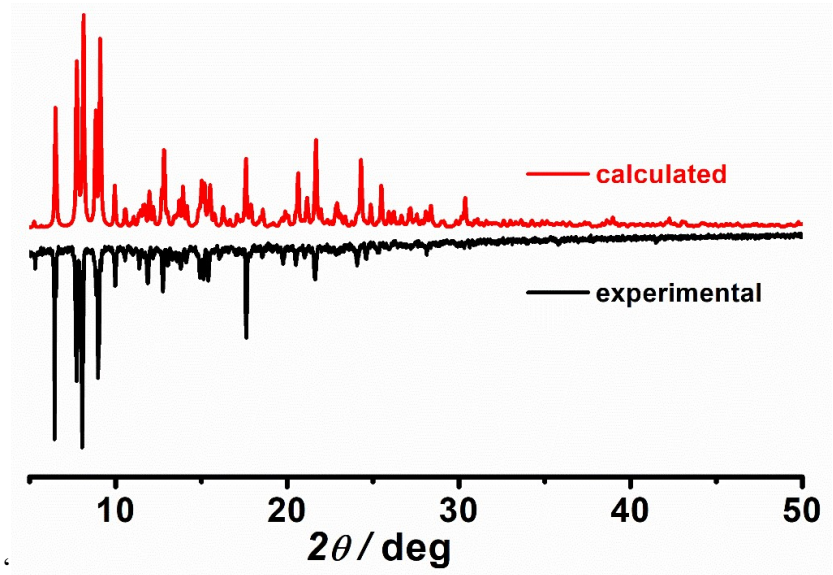

Figure S2. The powder X-ray diffraction pattern of **2** at room temperature.

Table S1. Crystal data and structure refinements for **1** and **2**.

	1	**2**
Molecular formula	$C_{37}H_{53}Co_2N_{12}O_6$	$C_{85}H_{108}Cl_2Co_4N_{24}O_8$
CCDC no	2156157	2156158
Formula weight	879.77	1900.57
Temperature / K	173(2)	173(2)
Wavelength / Å	0.71073	0.71073
crystal system	Triclinic	Triclinic
Space group	*P*-1	*P*-1
a / Å	10.9935(17)	13.743(2)
b / Å	11.9446(18)	18.029(3)
c / Å	17.140(2)	20.727(3)
α / deg	70.849(5)	69.604(5)
β / deg	86.836(5)	84.300(5)
γ / deg	71.907(5)	81.659(6)
V / Å^3	2018.3(5)	4756.1(13)
Z	2	2
D_{calc}, g/cm^3	1.448	1.327
μ / mm^{-1}	0.883	0.806
F (000)	922	1984
Goodness-of-fit on F^2	0.978	1.066
Final *R* indices [*I* >2*σ*(*I*)][a]	R_1 = 0.0737, wR_2 = 0.1837	R_1 = 0.0859, wR_2 = 0.2391
R indices (all data)[a]	R_1 = 0.1063, wR_2 = 0.2069	R_1 = 0.1435, wR_2 = 0.2672

[a]$wR_2 = [\Sigma[w(F_o^2–F_c^2)^2]/\Sigma[w(Fo^2)^2]]^{1/2}$, $R_1 = \Sigma||F_o|–|F_c||/\Sigma|F_o|$.

Table S2. Selected bond lengths (Å) and angles (deg) for **1**.

Co(III)		**Co(II)**	
Co(1)-N(1)	1.918(4)	Co(2)-O(3)	1.974(3)
Co(1)-N(2)	1.934(4)	Co(2)-O(4)	2.637(3)
Co(1)-N(3)	1.905(4)	Co(2)-N(5)	2.008(4)
Co(1)-N(4)	1.902(4)	Co(2)-N(6)	2.005(4)
Co(1)-N(9)	1.955(4)	Co(2)-N(7)	2.024(5)
Co(1)-N(11)	2.007(4)		
N(1)-Co(1)-N(2)	96.69(16)	N(6)-Co(2)-N(5)	103.12(15)
N(3)-Co(1)-N(1)	81.98(16)	N(5)-Co(2)-N(7)	105.61(17)
N(3)-Co(1)-N(4)	99.28(16)	N(6)-Co(2)-N(7)	103.98(17)
N(4)-Co(1)-N(2)	82.04(16)	O(3)-Co(2)-N(5)	124.94(15)
N(9)-Co(1)-N(11)	177.75(15)	O(3)-Co(2)-N(6)	116.82(15)
		O(3)-Co(2)-N(7)	99.95(16)

Table S3. Selected bond lengths (Å) and angles (deg) for **2**.

Co(III)				Co(II)			
Co(1)-N(1)	1.908(5)	Co(3)-N(13)	1.916(5)	Co(2)-O(3)	1.956(5)	Co(4)-O(7)	1.946 (8)
Co(1)-N(2)	1.927(4)	Co(3)-N(14)	1.926(5)	Co(2)-O(4)	2.581(9)	Co(4)-O(8)	2.692(13)
Co(1)-N(3)	1.916(5)	Co(3)-N(15)	1.906(5)	Co(2)-N(4)	2.016(5)	Co(4)-N(16)	1.973(6)
Co(1)-N(5)	1.903(5)	Co(3)-N(17)	1.916(5)	Co(2)-N(6)	2.021(5)	Co(4)-N(18)	2.015(6)
Co(1)-N(7)	1.969(5)	Co(3)-N(19)	1.971(5)	Co(2)-N(11)	2.014(5)	Co(4)-N(23)	2.034(6)
Co(1)-N(9)	1.985(5)	Co(3)-N(21)	2.016(5)				
N(1)-Co(1)-N(2)	95.8(2)	N(13)-Co(3)-N(14)	96.5(2)	N(11)-Co(2)-N(4)	105.6(2)	N(16)-Co(4)-N(18)	103.9(4)
N(1)-Co(1)-N(3)	81.9(2)	N(15)-Co(3)-N(13)	81.5(2)	N(11)-Co(2)-N(6)	105.7(2)	N(16)-Co(4)-N(23)	102.9(4)
N(5)-Co(1)-N(3)	100.3(2)	N(15)-Co(3)-N(17)	99.4(2)	N(4)-Co(2)-N(6)	104.0(2)	N(18)-Co(4)-N(23)	107.7(4)
N(5)-Co(1)-N(2)	81.9(2)	N(17)-Co(3)-N(14)	82.7(2)	O(3)-Co(2)-N(4)	117.3(2)	O(7)-Co(4)-N(16)	119.6(5)
N(7)-Co(1)-N(9)	178.9(2)	N(19)-Co(3)-N(21)	178.9(2)	O(3)-Co(2)-N(6)	123.6(2)	O(7)-Co(4)-N(18)	119.3(5)
				O(3)-Co(2)-N(11)	98.6(2)	O(7)-Co(4)-N(23)	101.8(3)

Table S4. Continuous shape measure (CShM) analyses for **1** and **2**. The lowest CShM value is highlighted.

Ideal Polyhedron	**1**	**2**	
	Co2	Co2	Co4
Pentagon (D_{5h})	30.047	30.542	30.409
Vacant octahedron (C_{4v})	7.261	6.868	7.763
Trigonal bipyramid (D_{3h})	4.951	4.566	5.749
Spherical square pyramid (C_{4v})	6.004	5.256	5.697
Johnson trigonal bipyramid J12 (D_{3h})	5.124	5.013	5.542

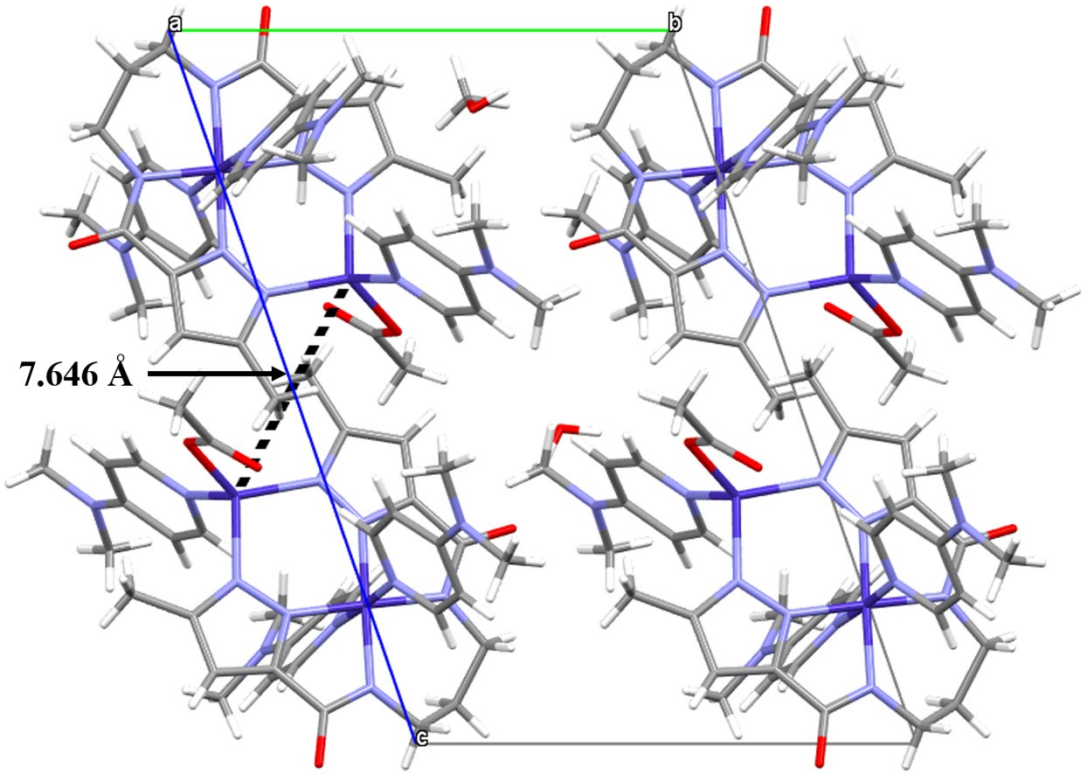

Figure S3. The packing diagram for complex **1** gives the shortest Co(II)···Co(II) distance of 7.646 Å.

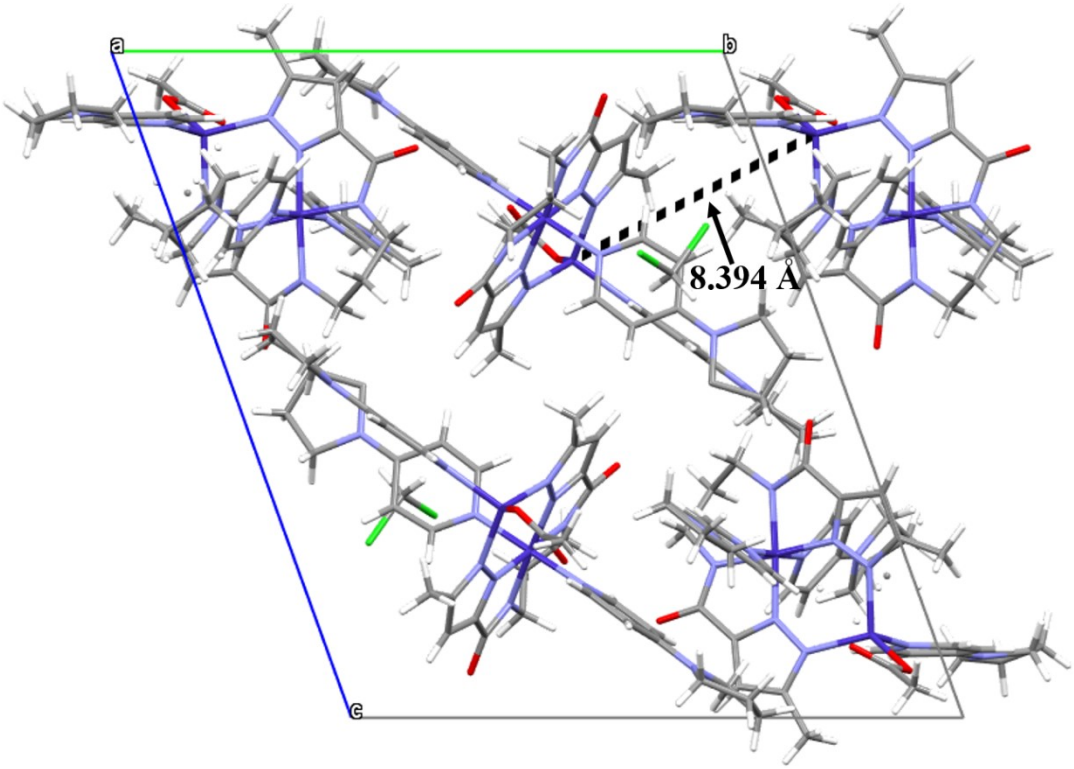

Figure S4. The packing diagram for complex **2** gives the shortest Co(II)···Co(II) distance of 8.394 Å.

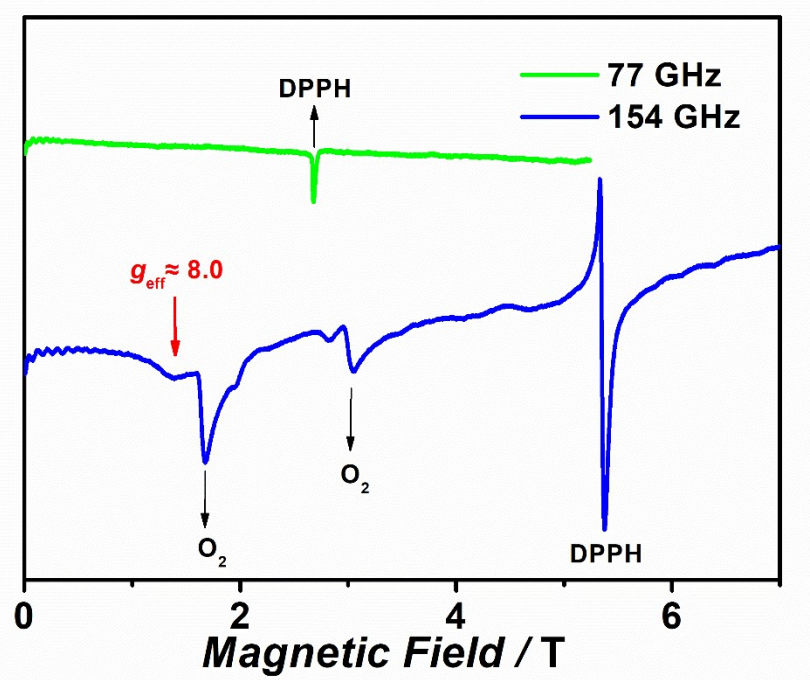

Figure S5. The HFEPR spectra of **1** at 2 K.

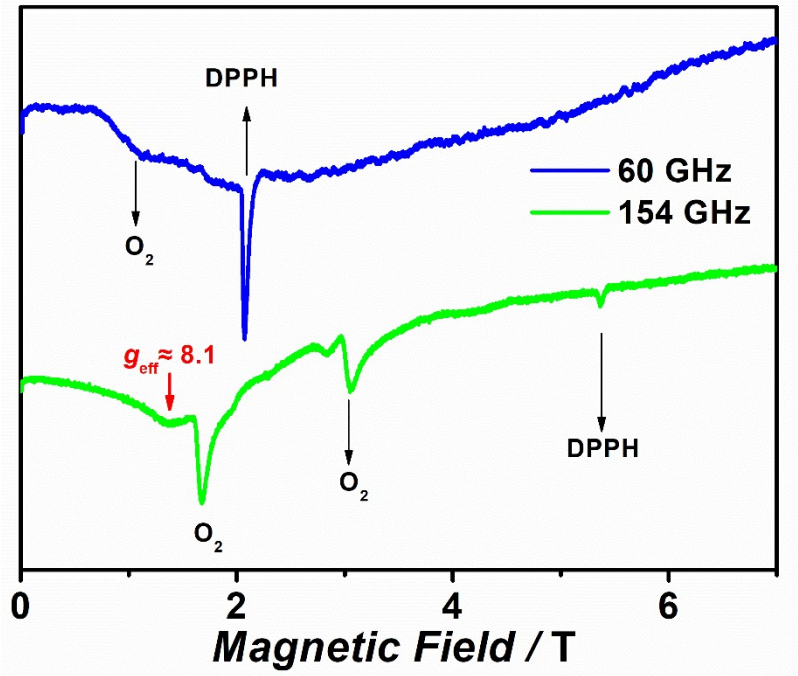

Figure S6. The HFEPR spectra of **2** at 2 K.

Table S5. Calculated values of ***D***, ***E***, and ***g*** for **1** and **2** using ORCA/CASSCF+NEVPT2.

Complex	D (cm^{-1})	E (cm^{-1})	g_{iso}	g_x	g_y	g_z
1	-24.64	-0.72	2.2607	2.1536	2.1722	2.4564
2-Co2	-20.37	-0.62	2.2498	2.1588	2.1766	2.4139
2-Co4	-15.70	-1.90	2.2485	2.1610	2.2088	2.3757

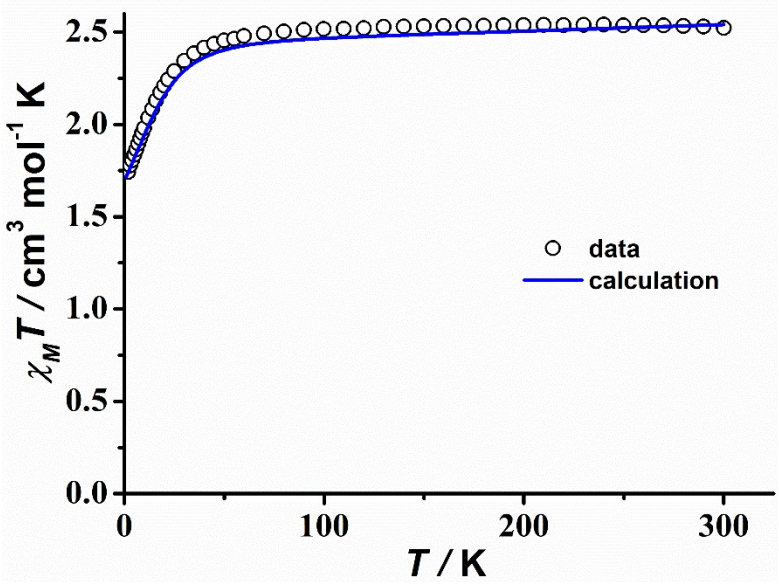

Figure S7. The theoretical (solid line) curves of magnetic susceptibilities of **1**.

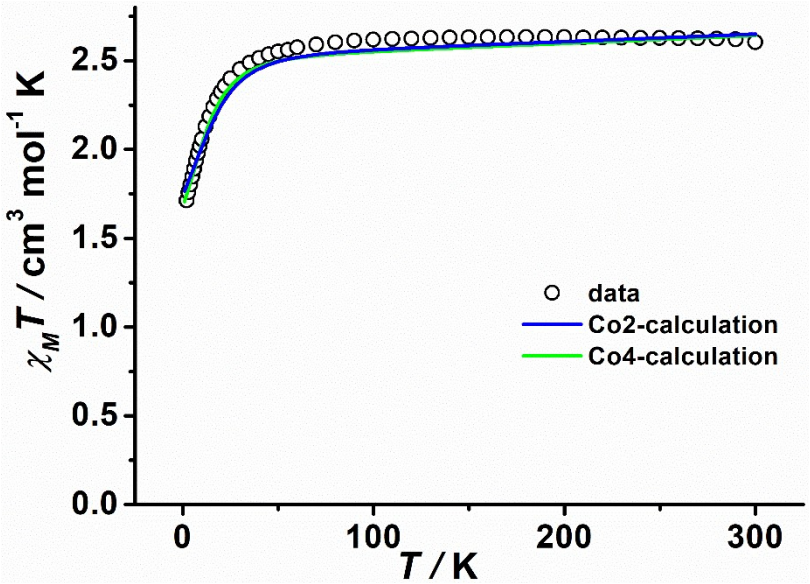

Figure S8. The theoretical (solid line) curves of magnetic susceptibilities of **2**.

Table S6. Calculated energy levels (cm^{-1}) and $\boldsymbol{g}$ (g_x, g_y, g_z) tensors of the lowest Kramers doublets (KDs) of the Co^{II} for **1** and **2** using ORCA/CASSCF+NEVPT2+SINGLE_ANISO.

1					**2-Co2**				
KDs	E/cm^{-1}	g_x	g_y	g_z	KDs	E/cm^{-1}	g_x	g_y	g_z
1	0.000	0.1866	0.1934	7.3444	1	0.000	0.1941	0.1980	7.2196
2	49.337	4.4860	4.1431	2.4749	2	40.797	4.5030	4.1455	2.4260
3	2522.007	4.6964	4.0604	1.5253	3	2823.737	4.5871	4.1819	1.5733
4	2642.787	0.2592	0.2753	4.6923	4	2937.620	0.1615	0.1788	4.8037

2-Co4				
KDs	E/cm^{-1}	g_x	g_y	g_z
1	0.000	0.7233	0.8273	7.0115
2	32.077	2.2884	3.5794	5.0365
3	3003.018	5.2138	3.6091	1.5857
4	3111.435	0.6715	0.7226	4.9337

Table S7. Individual contributions to *D*-tensor for **1** and **2** calculated using CASSCF/NEVPT2/ZORA-def2-TZVP(-f).

		1		**2-Co2**		**2-Co4**	
2*S*+1	**Root**	***D***	***E***	***D***	***E***	***D***	***E***
4	0	0.000	0.000	0.000	0.000	0.000	0.000
4	1	-39.537	0.046	-36.465	0.008	-31.358	-0.326
4	2	5.451	-6.004	7.300	-7.372	7.137	-7.790
4	3	5.244	6.538	5.747	5.611	4.024	2.544
4	4	2.922	-1.266	1.669	0.966	3.726	3.382
4	5	-0.283	-0.013	-0.212	0.002	-0.381	-0.037
4	6	0.111	-0.072	0.122	0.016	0.112	0.023
4	7	0.016	-0.011	0.012	0.000	0.018	-0.003
4	8	0.001	-0.001	0.001	0.000	-0.001	-0.000
4	9	-0.019	-0.000	-0.015	0.000	-0.025	0.001
2	0	-0.433	0.763	-0.491	0.561	-0.444	0.322
2	1	0.131	-0.555	0.161	-0.399	0.250	-0.259
2	2	0.388	-0.022	0.445	-0.012	0.494	-0.013
2	3	0.103	-0.001	0.025	0.002	0.023	-0.001
2	4	-0.005	0.007	0.044	0.004	0.038	-0.000
2	5	0.142	-0.010	0.047	0.017	0.121	0.006
2	6	4.349	-0.027	4.919	-0.030	4.412	0.041
2	7	-1.714	1.582	-1.924	0.417	-1.830	1.033
2	8	-2.232	-2.043	-2.261	-0.395	-2.301	-0.997
2	9	-0.258	0.368	-0.275	0.063	-0.258	0.081
2	10	0.685	-0.005	0.659	-0.021	0.385	0.044
2	11	0.104	0.013	0.218	-0.028	0.236	-0.034

2	12	0.317	0.003	0.181	-0.000	0.413	-0.010
2	13	-0.067	0.025	-0.015	0.005	-0.104	0.080
2	14	-0.085	-0.047	-0.094	-0.056	-0.059	-0.051
2	15	0.002	-0.008	-0.122	0.062	-0.041	0.039
2	16	-0.253	0.193	-0.112	0.055	-0.236	0.081
2	17	0.142	-0.001	0.101	0.000	-0.002	0.018
2	18	-0.014	-0.017	0.038	-0.002	0.119	-0.016
2	19	0.049	-0.023	-0.014	-0.012	0.055	-0.010
2	20	0.010	-0.002	0.003	-0.006	-0.051	-0.034
2	21	-0.006	-0.027	0.021	-0.004	0.080	-0.004
2	22	-0.741	0.698	-0.754	-0.382	-0.793	-0.767
2	23	-0.687	-0.660	-0.634	0.282	-0.406	0.397
2	24	-0.014	0.011	-0.026	0.004	-0.076	0.092
2	25	0.350	-0.005	0.352	-0.007	0.418	0.010
2	26	-0.002	-0.002	-0.001	-0.000	-0.001	0.002
2	27	-0.006	0.002	-0.003	0.000	-0.003	-0.004
2	28	-0.007	0.005	-0.003	0.002	-0.006	0.002
2	29	0.304	0.001	0.301	-0.002	0.260	0.019
2	30	-0.093	0.091	-0.104	0.089	-0.055	0.019
2	31	-0.089	-0.087	-0.097	-0.078	-0.096	-0.024
2	32	-0.010	-0.008	-0.007	-0.002	-0.010	-0.008
2	33	-0.011	0.013	-0.009	0.005	-0.012	0.006
2	34	0.000	0.001	0.000	-0.000	-0.000	-0.000
2	35	-0.000	-0.001	0.000	-0.000	0.000	0.000
2	36	-0.015	-0.015	-0.014	-0.014	-0.016	-0.004
2	37	-0.007	0.008	-0.005	0.005	-0.006	-0.002
2	38	-0.008	0.003	-0.014	0.007	-0.016	0.008
2	39	0.027	0.006	0.035	0.004	0.037	-0.002

Table S8. Energy levels (cm^{-1}) of ligand field multiplets for **1** and **2** calculated using CASSCF/ZORA-def2-TZVP(-f) in magnetic zero field.

	I	**2-Co2**	**2-Co4**
States	**Energy levels (cm^{-1})**	**Energy levels (cm^{-1})**	**Energy levels (cm^{-1})**
1	0.0	0.0	0.0
2	49.3	40.8	32.1
3	49.3	40.8	32.1
4	2522.0	2823.7	3003.0
5	2522.0	2823.7	3003.0
6	2642.8	2937.6	3111.4
7	2642.8	2937.6	3111.4
8	6136.7	6347.9	5512.0
9	6136.7	6347.9	5512.0
10	6293.0	6516.0	5652.6
11	6293.0	6516.0	5652.6

12	7281.2	7165.5	6818.3
13	7281.2	7165.5	6818.3
14	7375.1	7291.7	6955.8
15	7375.1	7291.7	6955.8
16	7964.3	8245.5	7941.1
17	7964.3	8245.5	7941.1
18	8052.6	8343.3	8034.2
19	8052.6	8343.3	8034.2
20	9553.8	9548.2	9717.7
21	9553.8	9548.2	9717.7
22	9665.7	9671.2	9833.3
23	9665.7	9671.2	9833.3
24	13158.8	12724.5	12919.5
25	13158.8	12724.5	12919.5
26	13180.0	12750.2	12947.9
27	13180.0	12750.2	12947.9
28	15991.0	16474.4	15852.4
29	15991.0	16474.4	15852.4
30	16825.1	17222.0	17176.5
31	16825.1	17222.0	17176.5
32	18584.8	18658.7	18413.3
33	18584.8	18658.7	18413.3
34	18883.8	18893.7	18813.6
35	18883.8	18893.7	18813.6
36	19577.0	19410.3	19571.5
37	19577.0	19410.3	19571.5
38	20472.5	20632.0	20659.6
39	20472.5	20632.0	20659.6
40	20788.8	21067.5	20908.8
41	20788.8	21067.5	20908.8
42	20837.7	21121.5	20955.5
43	20837.7	21121.5	20955.5
44	21150.6	21298.1	21192.4
45	21150.6	21298.1	21192.4
46	21718.9	21491.1	21292.1
47	21718.9	21491.1	21292.1
48	21810.0	21612.1	21389.4
49	21810.0	21612.1	21389.4
50	22398.8	22253.8	22409.6
51	22398.8	22253.8	22409.6
52	22595.8	22436.0	22576.6
53	22595.8	22436.0	22576.6
54	22907.1	23210.1	22752.8
55	22907.1	23210.1	22752.8

56	23819.6	23930.4	23879.4
57	23819.6	23930.4	23879.4
58	24230.6	24235.0	23997.9
59	24230.6	24235.0	23997.9
60	24615.2	24662.6	24513.4
61	24615.2	24662.6	24513.4
62	25134.8	25272.8	25005.0
63	25134.8	25272.8	25005.0
64	26603.1	26516.8	26206.9
65	26603.1	26516.8	26206.9
66	26917.9	26706.0	26732.9
67	26917.9	26706.0	26732.9
68	27281.4	27157.9	27578.0
69	27281.4	27157.9	27578.0
70	28017.9	27839.4	27912.7
71	28017.9	27839.4	27912.7
72	28214.1	28229.1	28162.1
73	28214.1	28229.1	28162.1
74	29390.2	29357.2	29584.7
75	29390.2	29357.2	29584.7
76	29886.1	29638.8	29876.0
77	29886.1	29638.8	29876.0
78	30496.0	30512.5	30129.3
79	30496.0	30512.5	30129.3
80	31010.0	30823.9	30829.0
81	31010.0	30823.9	30829.0
82	31239.3	31154.9	31054.4
83	31239.3	31154.9	31054.4
84	31442.3	31401.8	31485.8
85	31442.3	31401.8	31485.8
86	32048.7	31936.6	32269.5
87	32048.7	31936.6	32269.5
88	33992.5	33786.9	33443.3
89	33992.5	33786.9	33443.3
90	34774.5	34636.1	33865.4
91	34774.5	34636.1	33865.4
92	35409.7	35459.4	35426.4
93	35409.7	35459.4	35426.4
94	36585.2	36685.2	36156.7
95	36585.2	36685.2	36156.7
96	41060.2	40942.4	41016.7
97	41060.2	40942.4	41016.7
98	41521.9	41427.5	41377.5
99	41521.9	41427.5	41377.5

100	42177.5	42043.4	42007.1
101	42177.5	42043.4	42007.1
102	42678.8	42576.6	42571.6
103	42678.8	42576.6	42571.6
104	43331.1	43363.0	43284.2
105	43331.1	43363.0	43284.2
106	43716.6	43660.3	43723.1
107	43716.6	43660.3	43723.1
108	44683.4	44597.7	44343.7
109	44683.4	44597.7	44343.7
110	61163.3	61006.6	60999.7
111	61163.3	61006.6	60999.7
112	62749.1	62737.3	62600.0
113	62749.1	62737.3	62600.0
114	63128.3	63014.2	63077.5
115	63128.3	63014.2	63077.5
116	63987.8	63808.6	63583.6
117	63987.8	63808.6	63583.6
118	64505.1	64221.9	64463.5
119	64505.1	64221.9	64463.5

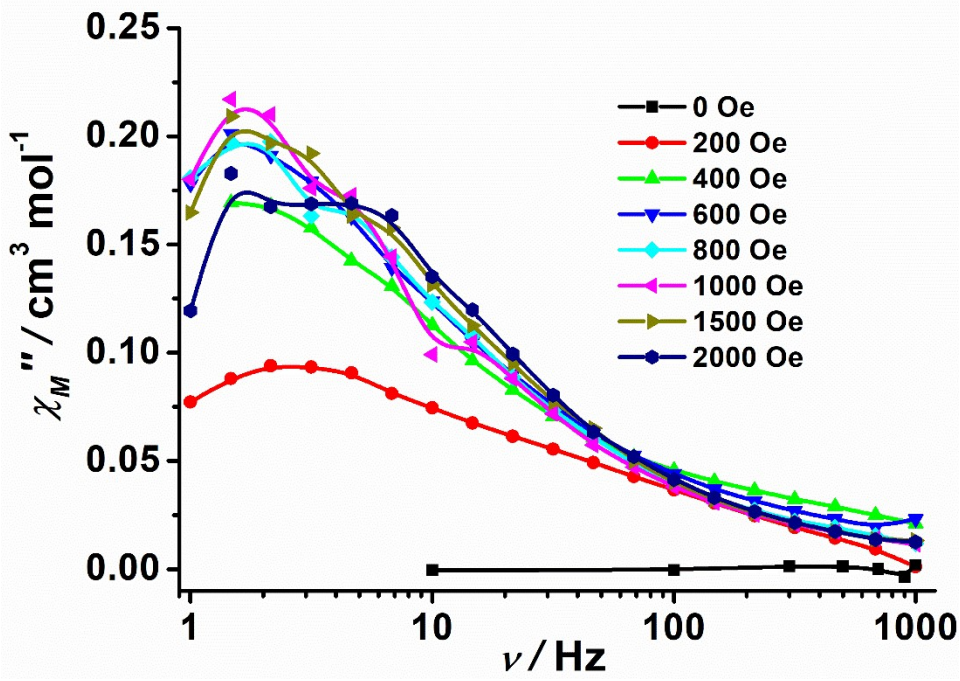

Figure S9. Frequency dependence of out-of-phase (χ_M'') ac susceptibility at 2.0 K under the different applied fields from 0 to 2000 Oe for **1**. The solid lines are for eye guide.

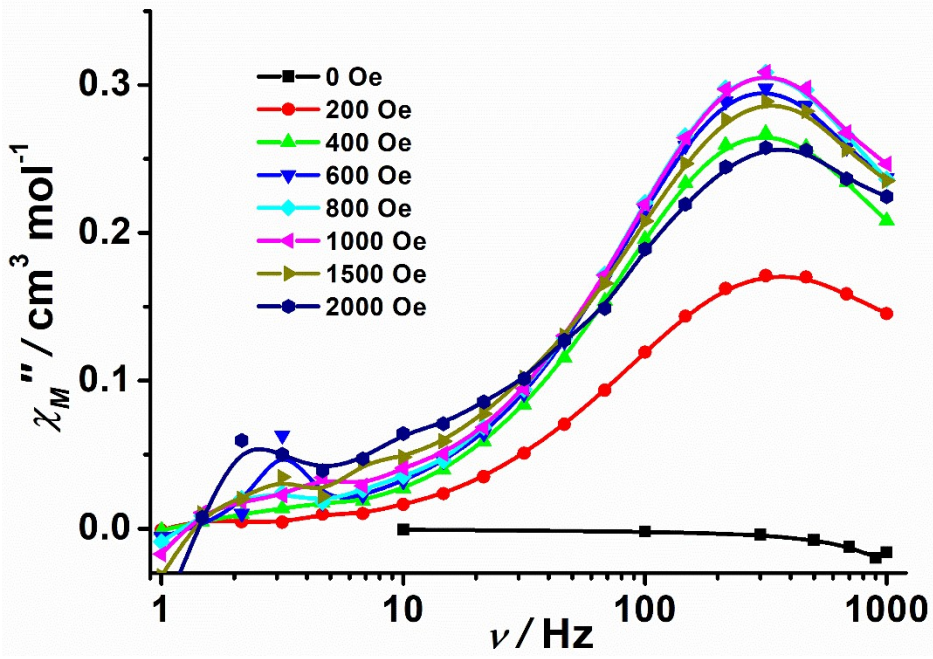

Figure S10. Frequency dependence of out-of-phase (χ_M'') ac susceptibility at 2.0 K under the different applied fields from 0 to 2000 Oe for **2**. The solid lines are for eye guide.

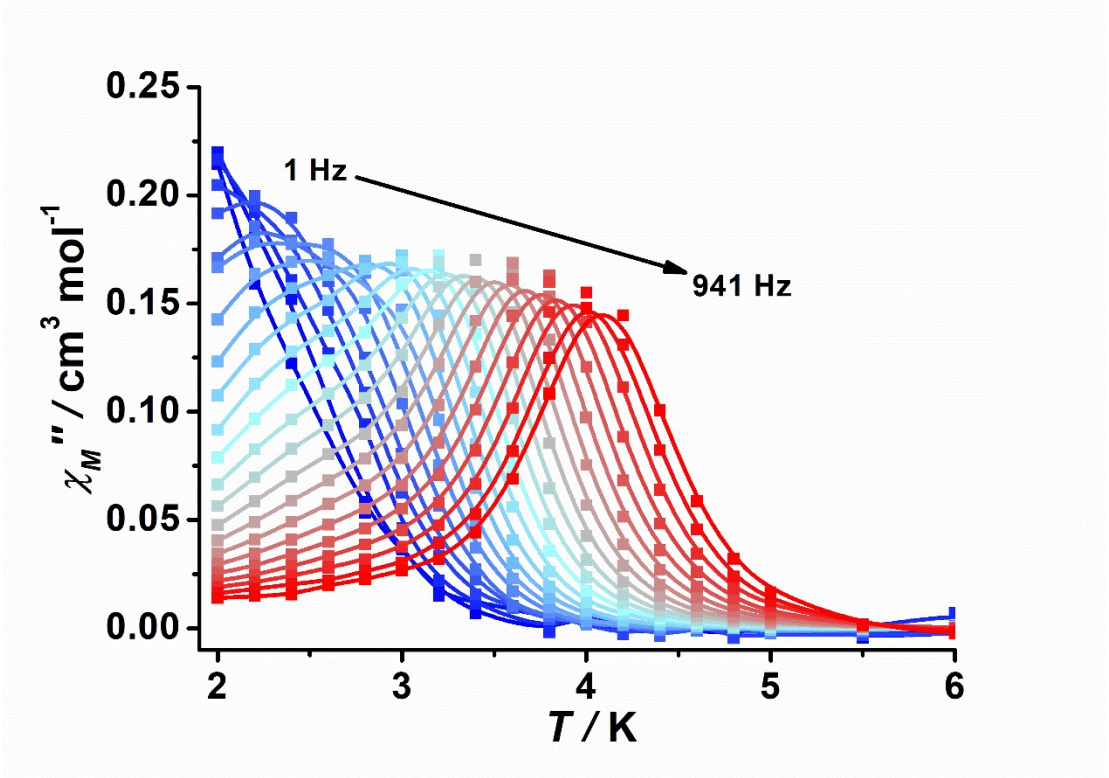

Figure S11. Temperature dependence of out-of-phase (χ_M'') ac susceptibility u under the 1000 Oe applied field for **1**. The solid lines are for eye guide.

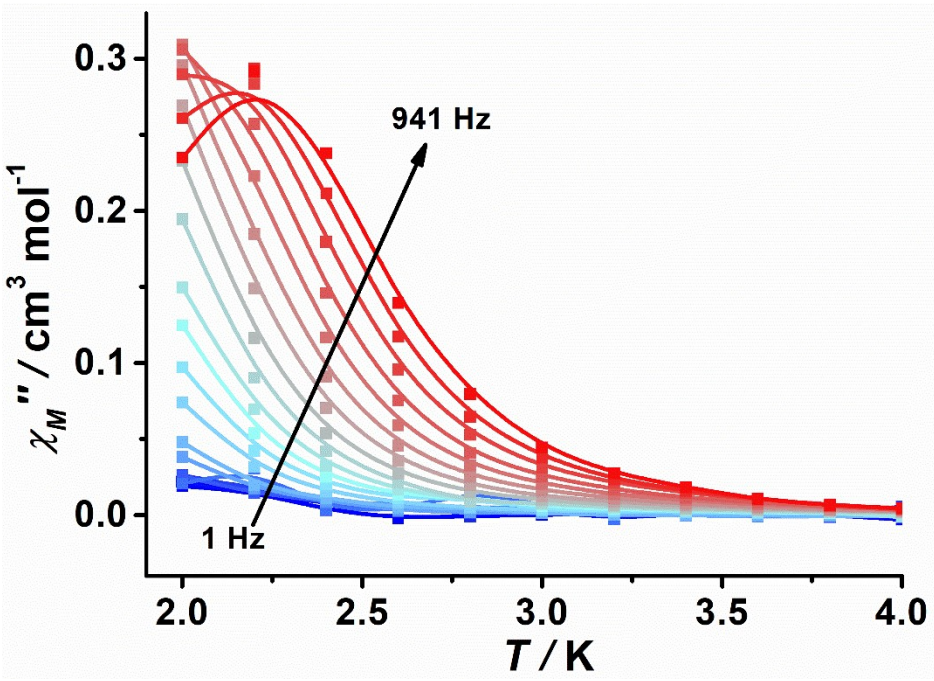

Figure S12. Temperature dependence of out-of-phase (χ_M'') ac susceptibility under under the 1000 Oe applied field for **2**. The solid lines are for eye guide.

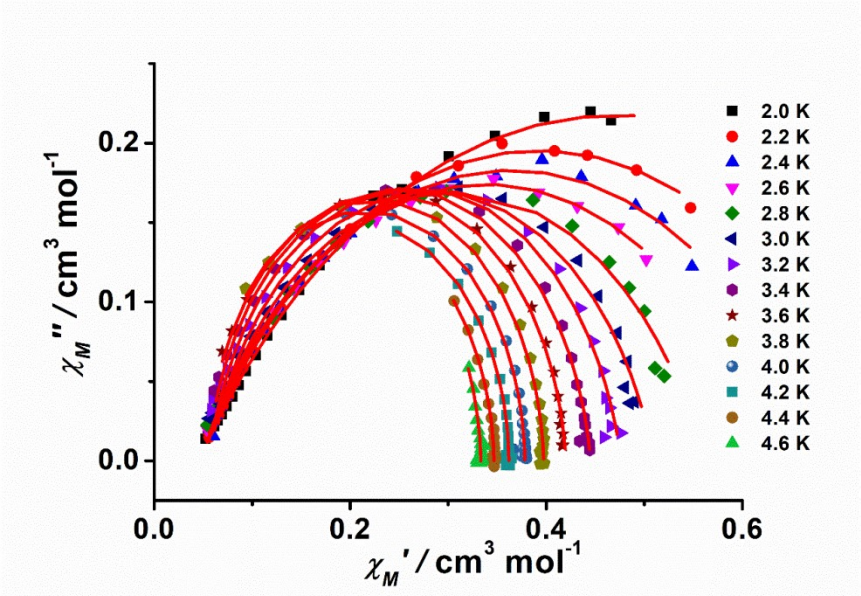

Figure S13. Cole-Cole plot obtained from the ac susceptibility data under the 1000 Oe applied field in the temperature range of 2.0-4.6 K for **1**.

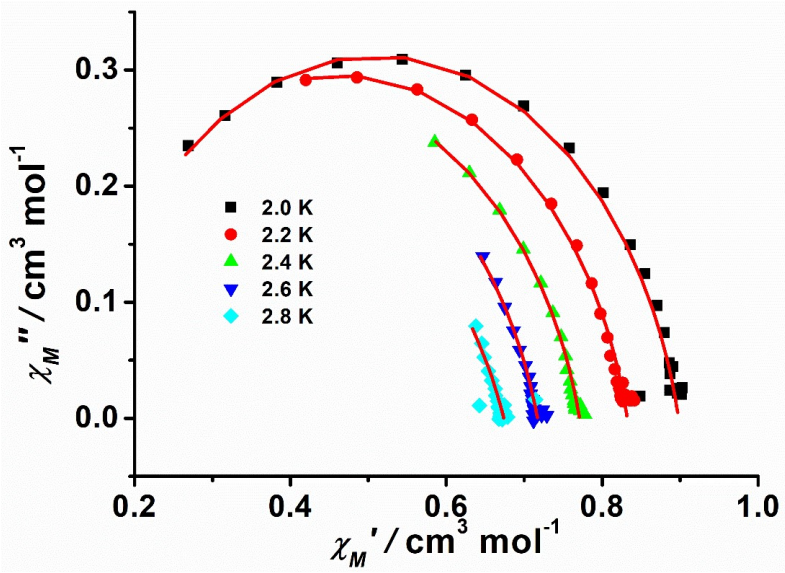

Figure S14. Cole-Cole plot obtained from the ac susceptibility data under the 1000 Oe applied field in the temperature range of 2.0-2.8 K for **2**.

Table S9. The parameters obtained by fitting Cole-Cole plot under the 1000 Oe applied field for **1**.

T / K	χ_S	χ_T	τ	a
2.0	0.045	0.90	0.14	0.40
2.2	0.047	0.74	0.057	0.34
2.4	0.046	0.68	0.035	0.34
2.6	0.046	0.63	0.022	0.32
2.8	0.051	0.56	0.013	0.25
3.0	0.055	0.51	0.0075	0.18
3.2	0.055	0.48	0.0041	0.13
3.4	0.054	0.44	0.0021	0.08
3.6	0.053	0.42	0.0010	0.05
3.8	0.053	0.40	0.00050	0.09
4.0	0.055	0.38	0.00025	0.02
4.2	0.058	0.36	0.00013	0.01
4.4	0.036	0.35	0.000063	0.02
4.6	0	0.33	0.000030	0.02

Table S10. The parameters obtained by fitting Cole-Cole plot under the 1000 Oe applied field for **2**.

T / K	χ_S	χ_T	τ	a
2.0	0.12	0.90	0.00049	0.14
2.2	0.097	0.83	0.00020	0.14
2.4	0.047	0.77	0.000076	0.15
2.6	0	0.71	0.000030	0.17
2.8	0	0.67	0.000013	0.23

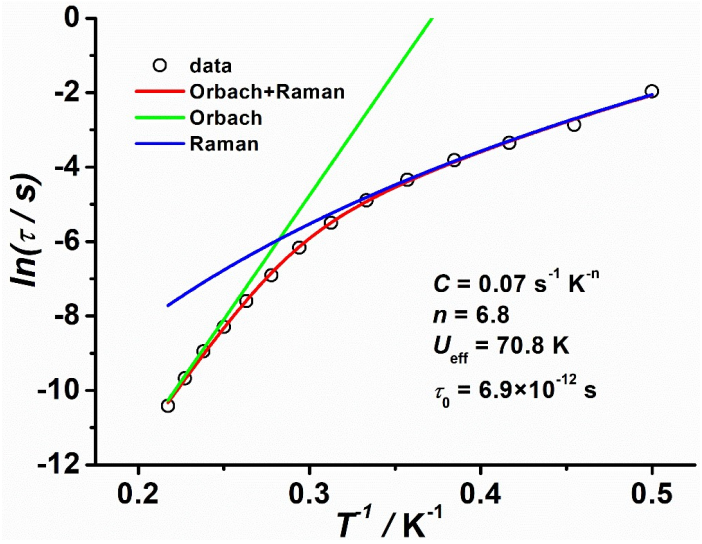

Figure S15. Relaxation time of the magnetization *ln(τ) vs* T^{-1} plot under the 1000 Oe applied field for **1**. The red line is the best fit to the relaxation time by the combination of Orbach and Raman processes. The blue and blue lines are representations for the Orbach and Raman processes, respectively.